ADVANCES IN ATMOSPHERIC SCIENCES, VOL. 43, APRIL 2026, 723–735

• **Original Paper** •

Hot Drought Increased the Occurrence Probability of the 2025 Los Angeles Destructive Wildfires※

Feng MA[1,2,3], Xing YUAN[*1,2,3], and Jason A. OTKIN[4]

[1]*School of Hydrology and Water Resources*, *Nanjing University of Information Science and Technology*, *Nanjing* 210044, *China*

[2]*State Key Laboratory of Earth System Numerical Modeling and Application*, *Institute of Atmospheric Physics*, *Chinese Academy of Sciences*, *Beijing* 100029, *China*

[3]*Key Laboratory of Hydrometeorological Disaster Mechanism and Warning of Ministry of Water Resources*, *Nanjing University of Information Science and Technology*, *Nanjing* 210044, *China*

[4]*Cooperative Institute for Meteorological Satellite Studies*, *Space Science and Engineering Center*, *University of Wisconsin-Madison*, *Madison*, *WI* 53706, *USA*

(Received 9 March 2025; revised 22 July 2025; accepted 28 July 2025)

ABSTRACT

The western Los Angeles (LA) wildfires of early January 2025 caused catastrophic social and environmental impacts, drawing widespread attention. This study investigates the characteristics of these wildfires and quantifies the influence of heat and drought on their likelihood using a copula-based Bayesian probability framework. The wildfires were characterized by burned area (BA) and intensity (fire radiative power, FRP). The criteria establishing the presence of "hot drought" conditions were identified using the 5-day Standardized Temperature Index (STI) and 75-day Standardized Precipitation Index (SPI), respectively. The wildfire outbreak began on 7 January 2025 and burned for more than six days, with the total burned area exceeding 245 km^2 and the cumulative FRP exceeding 41060 MW. Based on satellite-derived active fire observations from 2001 to 2025, we estimate that such large and intense wildfires during LA's rainy season represent a once-in-a-67-year event. The wildfires were largely driven by the combination of hot and dry conditions, which dried out soils and vegetation that had proliferated due to above-average precipitation in previous winter seasons, thereby providing abundant fuel. Our seasonal analysis reveals that extreme drought increased the probability of wildfires matching the 2025 intensity and BA by 54% and 75%, respectively. Hot drought further amplified these probabilities by 149% (intensity) and 210% (BA). These findings suggest an elevated risk of large wildfires under hot drought conditions, contributing to their expansion into the non-traditional fire season.

Key words: 2025 western Los Angeles wildfires, hot drought, copula-based probability, excessive vegetation growth, Santa Ana winds

Citation: Ma, F., X. Yuan, and J. A. Otkin, 2026: Hot drought increased the occurrence probability of the 2025 Los Angeles destructive wildfires. *Adv. Atmos. Sci.*, **43**(4), 723–735, https://doi.org/10.1007/s00376-025-5109-y.

Article Highlights:

- The 2025 western Los Angeles wildfires were a once-in-a-67-year event in terms of timing and severity.
- Hot drought conditions dried out abundant vegetation that had proliferated due to antecedent rainfall, creating fuel for the wildfires.
- Hot drought increased the risk of 2025-level wildfires by 2.8 and 4.4-fold (for intensity and burned area) over non-drought conditions.

1. Introduction

The western Los Angeles (LA) region (34°–34.5°N, 118°–119°W) experienced the ignition of multiple explosive wildfires (e.g., the Palisades and Eaton fires) on 7–8 January 2025, which burned over 50000 acres (~202 km^2) and destroyed more than 16000 structures (Qiu et al., 2025). Over 180000 people had to be evacuated, and the economic losses could exceed 250 billion US dollars. In addition, the large wildfires caused severe smoke pollution and threatened human physical and mental health (Qiu et al., 2025). There-

※ This paper is a contribution to the special topic on the 2025 Los Angeles Wildfires.

* Corresponding author: Xing YUAN
Email: xyuan2@mail.iap.ac.cn

fore, the 2025 wildfires have been reported as one of the most destructive fire events to have ever affected the western LA region.

These immense impacts inevitably brought the 2025 western LA wildfires to public attention, and also raised questions as to the underlying reasons and exceptional nature of the fires. Evidence is mounting that these wildfires resulted from multiple components, including human activities, landscape features, and meteorological conditions (Khorshidi et al., 2020; Brown et al., 2023; Qiu et al., 2025). Usually, wildfires in the western LA region occur in late summer and autumn (July through October) due to infrequent precipitation, high temperatures, and intense solar radiation (Fig. 1), which can lead to high evaporative demand and low-moisture fuels (Swain, 2021; Turco et al., 2023). Meanwhile, strong and dry Santa Ana winds during the fall and winter also contribute to western LA's large wildfires despite relatively low evaporative demand (Abatzoglou et al., 2018; Swain, 2021). Conditions are usually not conducive to drive large wildfires during mid-winter because it is the peak of western LA's rainy season, consistent with increases in relative humidity in response to relatively low temperatures and intermittent precipitation (Dong et al., 2022). However, if the onset of the rainy season is delayed and/or the winter is dry, the concurrent dryness and strong winds can increase the potential for large and fast-moving fires, as vegetation can be critically dry after the sustained dry and warm conditions typical of the summer and fall (Westerling et al., 2006; Dong et al., 2021; Gershunov et al., 2021).

A number of mechanisms linking wildfires to climatic

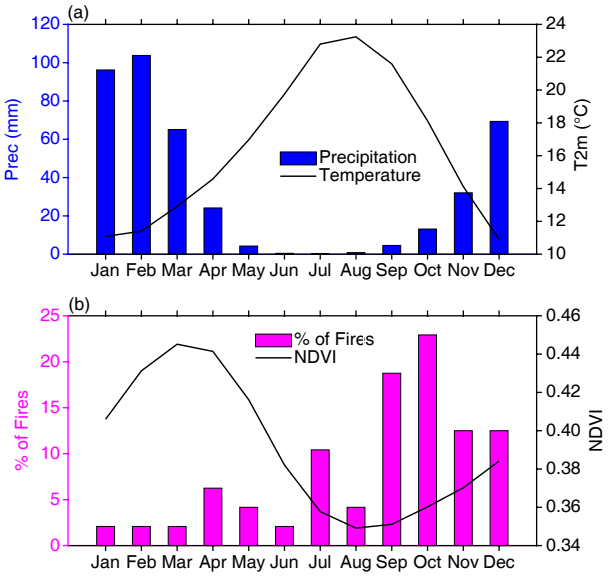

Fig. 1. The monthly (a) precipitation (Prec, mm; blue bars) and 2-m air temperature (T2m, °C; black lines) averaged over 1995–2024, and (b) mean normalized difference vegetation index (NDVI; black lines) and the occurrence percentage of fire events (%; bars) during 2001–24 in the western Los Angeles region (bounded by 34°–34.5°N, 118°–119°W). Here, the fire events were identified based on MODIS active fire data (see section 2.2.1).

factors have been suggested, including precipitation deficits, high temperatures, and large vapor pressure deficits (Westerling et al., 2006; Seager et al., 2015; Littell, 2018). In fact, some recent reports also revealed that the combination of Santa Ana winds and hot and dry weather created the perfect conditions for the rapid spread of the 2025 LA wildfires (Qiu et al., 2025). However, the quantitative characteristics of these wildfires and their dependence on hot and dry conditions have not been fully explored. Thus, this study aims to explore how and to what extent the hot and dry conditions contributed to the extremely rare wildfires from a probabilistic perspective. The remainder of this paper is organized as follows. Section 2 introduces the data and methods used in this study. Section 3 presents the spatiotemporal evolution of the 2025 western LA wildfires and quantifies the contribution of drought and hot conditions. Section 4 discusses the possible impacts of vegetation abundance and Santa Ana winds, and, finally, section 5 draws the main conclusions of the study.

2. Data and methods

2.1. *Datasets*

Daily satellite-based precipitation during 1995–2025 from the Climate Hazards Group InfraRed Precipitation with Station data (CHIRPS) with a spatial resolution of 0.05° × 0.05° (Funk et al., 2014) was used to help assess drought conditions. Other meteorological data, including 2-m air temperature (T2m) and dew point temperature (Tdew), evapotranspiration (ET), 10-m zonal and meridional winds, and soil moisture (SM, 0–7 cm and 7–28 cm), at an hourly scale during 1995–2025 were obtained from the fifth generation European Centre for Medium-Range Weather Forecasts (ECMWF) Land Surface Reanalysis (ERA5-Land, Muñoz-Sabater et al., 2021). The spatial resolution of the ERA5-Land datasets is 0.1° × 0.1°, and all hourly variables were aggregated into daily scales. The daily relative humidity (RH) was then estimated by daily T2m and Tdew (Alduchov and Eskridge, 1996). Although reanalysis products are an imperfect representation of reality, assessments of the ERA5-Land dataset have demonstrated that the product performs well in reproducing temperature extremes and soil moisture dynamics across the United States (Sheridan et al., 2020; Beck et al., 2021; Muñoz-Sabater et al., 2021).

Fire events were detected using the Terra and Aqua MODIS (MODerate resolution Imaging Spectroradiometer) daily active fire data (MOD14 and MYD14, Collection 61) between January 2001 and January 2025, as provided by the Fire Information Resource Management System (FIRMS). The dataset includes the locations of active fire hotspots and their intensity (i.e., Fire Radiative Power, FRP) with a 1-km spatial resolution, which represent the centroid of a 1-km^2 pixel with one or more fires that were flagged by the MODIS MOD14/MYD14 Fire and Thermal Anomalies algorithm (Giglio et al., 2003, 2016). The MODIS active fire product was used in this study because it provides both near-real-

time active fire locations and a long-term climatology necessary to compute probabilities, justifying its widespread use in global and regional fire detection and mapping (Hawbaker et al., 2008; Libonati et al., 2022; Shi et al., 2024). The MODIS active fire product can capture large fires well across the United States with detection rates exceeding 82%, but might miss small and low-intensity fires (Hawbaker et al., 2008; Fusco et al., 2019). This tendency may result in the underestimation of burned area and fire intensity, an imperfection deemed acceptable in our study, as our focus is on large wildfires, considering their profound ecological impacts and the robust active fire detection reliability of MODIS (Hawbaker et al., 2008). In southern California, large wildfires accounted for the majority of the total burned area and were strongly linked to extreme fire weather conditions (Dong et al., 2022). In contrast, small fires were more sensitive to human ignitions (Dong et al., 2022) and thus fall outside the scope of this study.

The normalized difference vegetation index (NDVI) was used to examine vegetation growth and fuel availability (Hernández Ayala et al., 2021). The NDVI was obtained from the MODIS Terra (MOD13C1) and Aqua (MYD13C1) databases with a spatial resolution of 0.05° × 0.05° and a temporal resolution of 16 days. An 8-day NDVI time series was then developed by merging the two 16-day satellite-based products (Wang et al., 2011), which has been widely used in climate, ecosystem, and natural resources management studies (Hernández Ayala et al., 2021; Liu et al., 2022; Burton et al., 2024).

For the purpose of establishing a connection with fire characteristics, all meteorological variables and NDVI were averaged over the study region in this study. The anomalies (or percentiles) of meteorological variables and NDVI were estimated with respect to the 1995–2024 and 2001–24 climatologies, respectively, considering their seasonal cycle.

2.2. *Methods*

2.2.1. *Fire analysis*

The characterization of fires was assessed by the burned area (BA) and FRP, representing the extent and intensity of fires. First, the start and end dates of the fires were identified based on the MODIS daily active fire hotspots. Here, only the vegetation fire hotpots (fire type=0) with a high confidence level (>80%) and FRP > 10 MW were considered. An active fire mask was developed for each fire, and then the BA and cumulative intensity were calculated at the end of the event. Despite the underestimation of the true fire severity, the satellite-derived fire detections provide valuable insight into the fire severity (Giglio et al., 2016). In this study, considering the locations of the 2025 wildfires, our analysis focused on the region bounded by 34°–34.5°N, 118°–119°W, which was referred to as the western LA region.

2.2.2. *Drought and hot conditions*

We used the Standard Precipitation Index (SPI) and Standard Temperature Index (STI) to identify and assess drought and hot conditions, respectively (McKee et al., 1993; Feng et al., 2019; Hao et al., 2021). In this study, the SPI and STI were calculated at a daily resolution. To obtain the optimal accumulated scales of SPI and STI, we estimated Pearson correlation coefficients between fire characteristics (i.e., BA) and SPI over 30–90 days and STI over 5–30 days. It can be found that the SPI at a 75-day scale and STI at a 5-day scale exhibited the highest correlation with BA (Fig. 2). Therefore, we adopted the 75-day SPI and 5-day STI that were estimated by summing precipitation from the preceding 74 days to the current day and averaging temperature from the preceding 4 days to the current day, respectively. For a given day, these two series were fitted to a marginal distribution (e.g., gamma distribution), and then transformed into a standard normal distribution to obtain the SPI and STI, respectively (McKee et al., 1993; Hao and AghaKouchak, 2013; Ma et al., 2019; Yang et al., 2025). Dry conditions were said to exist if SPI < –0.5, and a hot drought was present if SPI < –0.5 and STI > 0.5 (Svoboda et al., 2002).

2.2.3. *The relationship between fires and hot and drought conditions*

We used the copula method to assess the dependency between fire characteristics (BA and FRP) and dry and hot conditions (SPI and STI). The copula method can connect two or more variables with different marginal distributions, and has been widely used for drought and wildfire analysis (Li et al., 2023; Ma and Yuan, 2024; Ma et al., 2024). Several marginal distributions, including the normal, Generalized Extreme Value (GEV), Extreme Value (EV), Gaussian, and

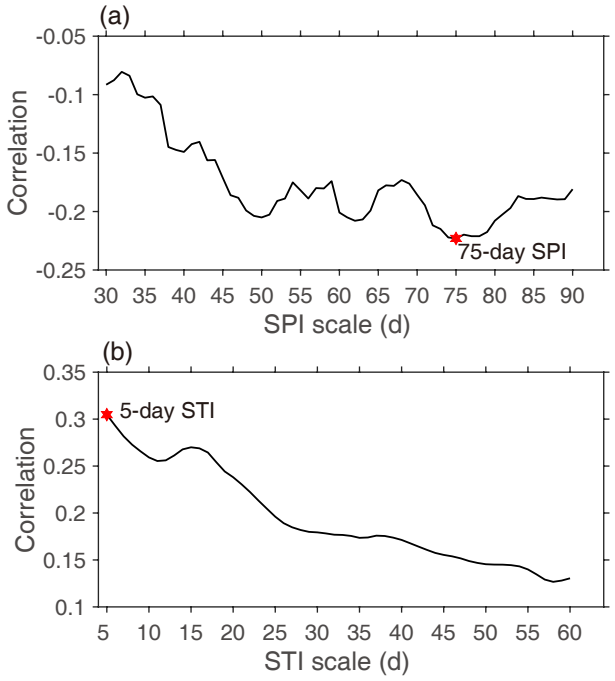

Fig. 2. The correlation coefficients between burned area and (a) SPI at 30–90-day scales and (b) STI at 5–60-day scales during the fire period. The red hexagons denote the timescale with the highest correlation.

empirical distributions, were tried to fit the log (BA), log (FRP), SPI, and STI series, and the most appropriate distribution for each variable was selected based on the Kolmogorov-Smirnov test. For the bivariate joint distribution, five copula functions, including Gaussian, Clayton, Gumbel, Frank, and t, were selected as candidates and then ranked based on their performance in the Maximum Likelihood (MLE), Akaike Information Content (AIC), Bayesian Information Criterion (BIC), Root-Mean-Square Error (RMSE), and Nash-Sutcliffe Efficiency (NSE) tests (Sadegh et al., 2017; Ballarin et al., 2021). The MLE test focuses on minimizing the residuals between model simulations and observations, the AIC considers the model complexity, and the BIC further takes into account the number of observations. The copula function that most frequently ranked first across these metrics was adopted as the optimal copula model. The C-vine copula function, characterized by its relatively simple structure and robust performance (Wu et al., 2021; Jiang et al., 2023), was then utilized to construct the trivariate joint distribution based on the AIC and BIC tests.

To assess the impact of drought and hot conditions on fires, we further estimated the probabilistic response of fires under different conditions from a statistical perspective. In this study, we particularly focused on the occurrence probability of fires like the 2025 wildfires, which were defined as $P[\log(BA_{area})>\log(BA_{2025})]$ or $P[\log(FRP_{intensity})>\log(FRP_{2025})]$, where BA_{area} and $FRP_{intensity}$ indicate BA and FRP, BA_{2025} and FRP_{2025} denote the BA and FRP of the 2025 wildfires, respectively. Following Ribeiro et al. (2020) and Hao et al. (2021), the conditional probability of fires with BA of the 2025 wildfires given non-dry, individual dry, and hot drought conditions can be expressed as:

$$\begin{aligned} &P[\log(BA_{area}) > \log(BA_{2025})|SPI_D > -0.5] \\ &= \frac{P[\log(BA_{area}) > \log(BA_{2025}), SPI_D > -0.5]}{P(SPI_D > -0.5)} \\ &= \frac{1 - P(SPI_D < -0.5) - P[\log(BA_{area}) < \log(BA_{2025})] + C[\log(BA_{area}) < \log(BA_{2025}), SPI_D < -0.5]}{1 - P(SPI_D < -0.5)}, \end{aligned} \tag{1}$$

$$\begin{aligned} P[\log(BA_{area}) > \log(BA_{2025})|SPI_D < spi_{2025}] &= \frac{P[\log(BA_{area}) > \log(BA_{2025}), SPI_D < spi_{2025}]}{P(SPI_D < spi_{2025})} \\ &= 1 - \frac{C[\log(BA_{area}) < \log(BA_{2025}), SPI_D < spi_{2025}]}{P(SPI_D < spi_{2025})}, \end{aligned} \tag{2}$$

and

$$\begin{aligned} &P[\log(BA_{area}) > \log(BA_{2025})|SPI_D < spi_{2025}, STI_H > sti_{2025}] \\ &= \frac{P[\log(BA_{area}) > \log(BA_{2025}), SPI_D < spi_{2025}, STI_H > sti_{2025}]}{P(SPI_D < spi_{2025}, STI_H > sti_{2025})} \\ &= 1 - \frac{C[\log(BA_{area}) < \log(BA_{2025}), SPI_D < spi_{2025}] - C[\log(BA_{area}) < \log(BA_{2025}), SPI_D < spi_{2025}, STI_H < sti_{2025}]}{P(SPI_D < spi_{2025}) - C(SPI_D < spi_{2025}, STI_H < sti_{2025})}, \end{aligned} \tag{3}$$

where C denotes the multivariate copula joint cumulative probability distribution, SPI_D and STI_H indicate SPI and STI, and spi_{2025} and sti_{2025} denote the actual SPI and STI values during the 2025 wildfires, respectively. Similarly, the conditional probability of FRP under different conditions can be estimated by $P[\log(FRP_{intensity})>\log(FRP_{2025})|SPI_D>-0.5]$, $P[\log(FRP_{intensity})>\log(FRP_{2025})|SPI_D<spi_{2025}]$, and $P[\log(FRP_{intensity})>\log(FRP_{2025})|SPI_D<spi_{2025}, STI_H>sti_{2025}]$, respectively. Then, the difference between Eq. (2) and Eq. (1) indicates the impact of drought, and the difference between Eq. (3) and Eq. (2) indicates the additional impact of hot drought, as opposed to drought impact alone. An intensified impact of extreme conditions on fires is expected to cause an increased conditional probability. The above copula-based Bayesian probability framework has been widely used to study the impact of drought and/or hot events on vegetation and wildfires (Hao et al., 2021; Ma et al., 2024).

3. Results

3.1. *Overview of the 2025 Los Angeles wildfires*

Figure 3 displays the satellite imagery provided by the FIRMS, showing the active fire locations in LA during 7–12 January 2025. The first wildfire erupted near the Pacific Palisades (i.e., Palisades Fire) on 7 January 2025, and spread quickly westward along the Pacific Coast Highway toward Malibu on 8 January. Further inland, another destructive fire (i.e., the Eaton Fire) ignited near Altadena, north of downtown LA, and grew rapidly on 8 January. Meanwhile, several major fires (e.g., Hurst Fire) also occurred in the San Fernando Valley. These large wildfires persisted from 7 January to 12 January, burning for more than 6 days. As of 12 January, several small fire hotspots were still active.

Figure 4 shows the total BA and intensity (FRP) of the

2025 wildfires in comparison to previous wildfires in the western LA region. In total, 133 fires were detected from January 2001 to January 2025 in the western LA region, with 36 events occurring in the winter season (December–February). Though the largest fires occurred in 2003 and 2009, large wildfires have become more frequent during the past decades, which has been attributed to climate warming (Abatzoglou and Williams, 2016; Brown et al., 2023; Turco et al., 2023). The BA of the 2025 wildfires was over 245 km^2, and the cumulative intensity was about 41 060

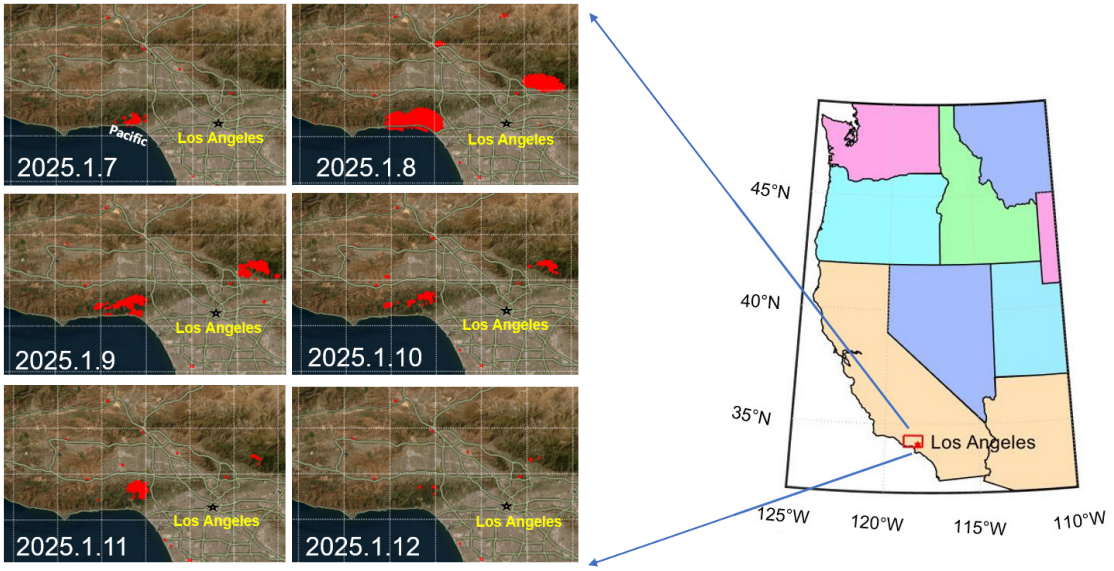

Fig. 3. The spatiotemporal evolution of the wildfires in the western Los Angeles (LA) region during 7–12 January 2025 (data source: Fire Information for Resource Management System, FIRMS). Red shadings denote fire detections. The red rectangle on the right map denotes the western LA region (34°–34.5°N, 118°–119°W) used for the quantitative analysis.

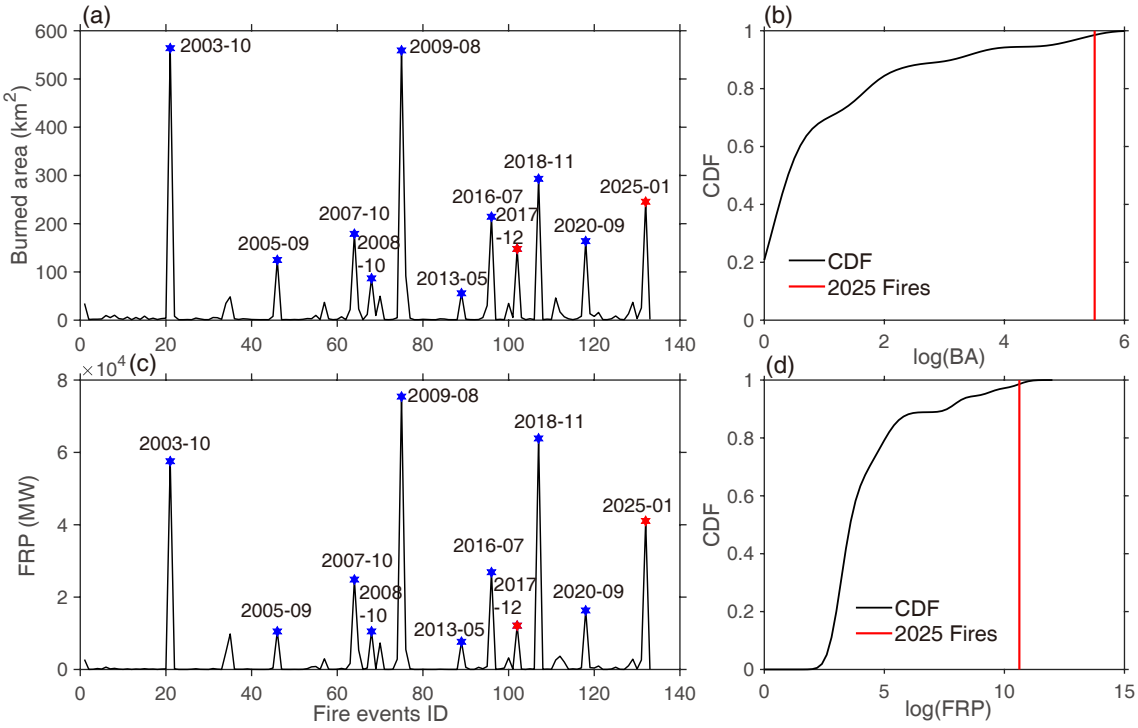

Fig. 4. The (a) Burned Area (BA, km^2) and (c) Fire Radiative Power (FRP, MW) for each wildfire event from January 2001 to January 2025, and the cumulative distribution function (CDF) of the (b) log (BA) and (d) log (FRP) for fires that occurred in winter season. Here, fires with BA >1 km^2 were considered. Blue hexagons denote the very large wildfires with BA ⩾ 50 km^2 that occurred in LA's fire-prone season, and red hexagons denote very large fires in the non-traditional fire season, including the 2025 wildfires.

MW (Figs. 4a, c). The 2025 wildfires ranked as the fourth largest and most intense fire event since 2001, surpassed only by the 24–29 October 2003, 27 August–7 September 2009, and 9–14 November 2018 fires. In spite of its relatively small BA and intensity compared to the three large wildfires, the 2025 wildfires were exceptional in terms of their destructive effects and the speed at which the fires developed (Qiu et al., 2025). In addition, we also note that a majority of dangerous wildfires occurred during the summer and autumn, coincident with scarce precipitation and high temperatures (Fig. 1). However, the 2025 wildfires occurred in midwinter when large wildfires are rare due to the climatologically wetter and cooler meteorological conditions, spanning a winter season characterized by mean BA of 8.24 km^2 and mean FRP of 574 MW over 2001–24. The BA (FRP) of the 2025 wildfires was approximately 30-fold (72-fold) larger than the mean BA (FRP) of fires in the winter climatology, constituting the largest observed values since 2001. We further fitted the log (BA) and log (FRP) of fires in the winter season to Kernel probability distributions to estimate the return period of the wildfires (Figs. 4b, d). The results indicate that the 2025 wildfires were about a 1-in-67-year and 1-in-68-year event during the winter in terms of their BA and intensity, respectively.

3.2. *Linking the 2025 Los Angeles wildfires to hot drought*

To further explore the drivers affecting the 2025 wildfires, we analyzed the temporal evolution of meteorological and vegetation conditions preceding the fires (Fig. 5). During the pre-fire and active fire periods (i.e., from December 2024 to mid-January 2025), the temperature was above normal, with a maximum anomaly of 4.18°C and a mean anomaly of 2.57°C (Fig. 5a). The summer of 2024 was also marked by numerous high temperature episodes. Meanwhile, the precipitation was lower than the climatological mean values, with rainfall amounts reaching zero or near-zero values from May 2024 to mid-January 2025 (Fig. 5b). The high evaporative demand drove high ET, which was consistently higher than precipitation (Figs. 5b, c). The persistent drought combined with warm temperatures induced rapid soil moisture decline since September 2024 (Fig. 5d). Conse-

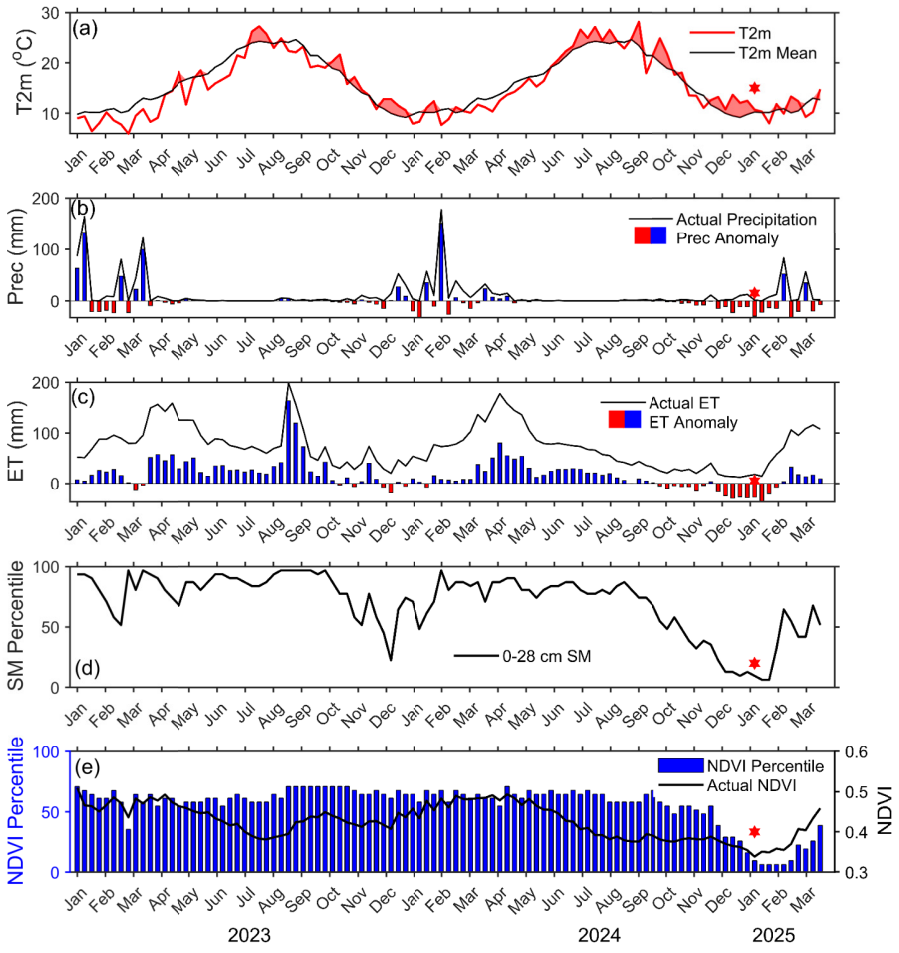

Fig. 5. Temporal evolution of the 8-day (a) 2-m air temperature (T2m, °C); (b) precipitation (Prec, mm); (c) evapotranspiration (ET, mm); (d) soil moisture (SM) percentile (%); (e) NDVI and its percentile (%) averaged over the analysis region from January 2023 to March 2025. Red hexagons denote the 2025 wildfire event.

quently, the vegetation vigor slowed down, as evidenced by the declining NDVI (Fig. 5e), leading to lower fuel moisture and the accumulation of dry fuels. It is noteworthy that the late winters of 2023 and 2024 were wetter than normal (Fig. 5b). The antecedent above-average rainfall fostered vegetative growth (Fig. 5e), resulting in abundant plant biomass and denser foliage (e.g., higher NDVI percentile), which later became available fuels for wildfires after sustained dry and warm conditions occurred from the summer of 2024 through early-January of 2025 (Khorshidi et al., 2020; Hernández Ayala et al., 2021). The concurrence of fire-prone weather and ample dry fuels contributed to the rapid spread, large BA, and intensity of the 2025 wildfires.

The above analysis confirms that the 2025 wildfires were largely driven by hot drought conditions. During the fire period, the mean SPI and STI were –1.57 and 1.03, corresponding to occurrence probabilities of < 6% and < 15% respectively. The quantitative indices further indicate the presence of extremely dry and hot conditions (i.e., hot drought). We thus quantified the impact of individual drought and hot drought on the fires via a copula-based Bayesian probability framework (see section 2.2.3). Figure 6 shows the scatterplots of SPI-STI, log(BA)-SPI, log(BA)-STI, and log(BA)-SPI-STI correlations, and the conditional probabilities of different levels of wildfires given different dry and/or hot conditions. A negative correlation existed for log(BA)-SPI (r=–0.22, p<0.01), while log(BA)-STI showed a positive correlation (r=0.30, p<0.001). Here, r is the Pearson correlation coefficient, and p denotes the significance level. The results indicate an increase in fire BA with the increased severity of drought and hot conditions. The conditional probability of wildfires with BA like the 2025 wildfires (BA=245 km^2) under actual drought conditions, i.e., $P[\log(BA_{area})>5.5|SPI_D\leqslant-1.57]$, was 14.14%, while the conditional probability given non-dry conditions, i.e., $P[\log(BA_{area})>5.5|SPI_D>-0.5]$, was 8.06%. This indicates that extreme drought during the pre-fire and fire periods increased the conditional probability of fires with BA similar to the 2025 wildfires by 75%. The conditional probability of the wildfires under the hot drought conditions, i.e., $P[\log(BA_{area})>5.5|SPI_D\leqslant-1.57, STI_H>1.03]$, was 43.85%, which was higher than that under the individual drought condition. The hot drought further increased the occurrence probability of the 2025 wildfires by 210%, compared with that under individual drought conditions

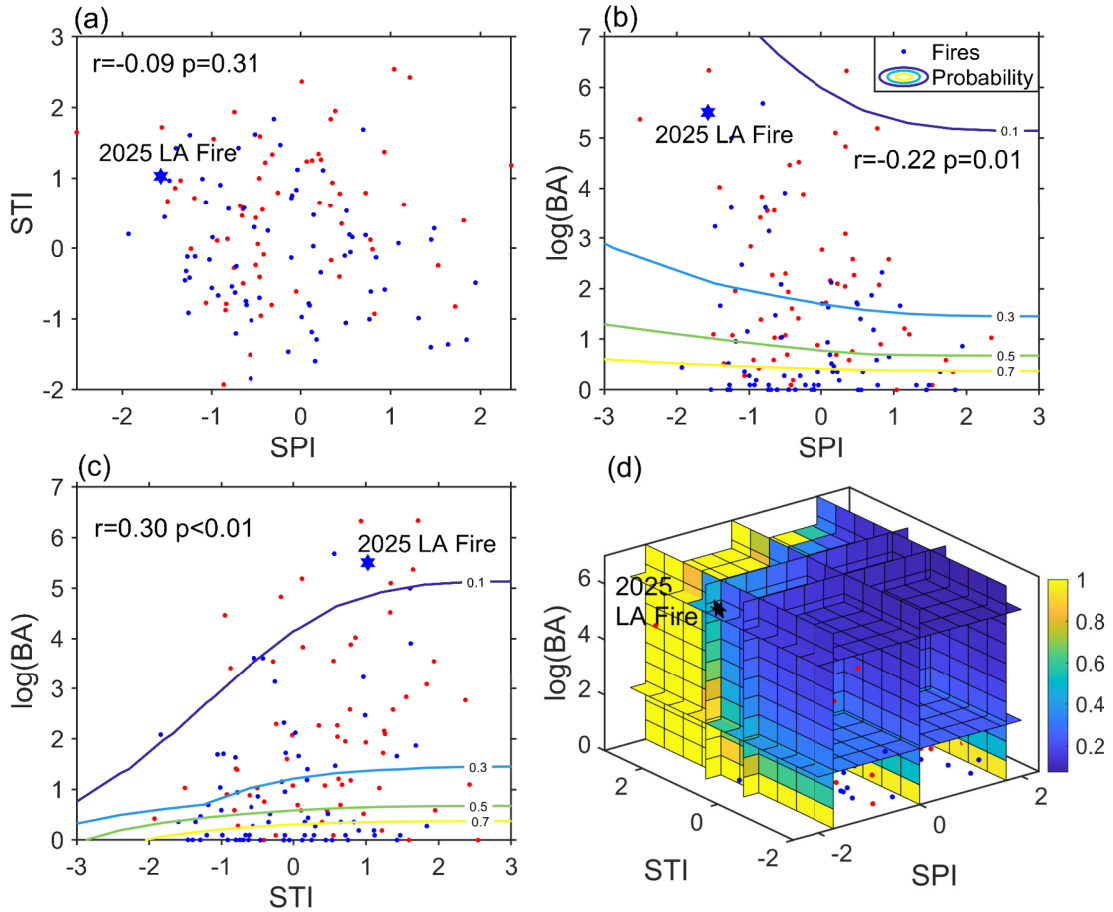

Fig. 6. Scatterplots of SPI, STI, and burned area (BA) for detected fire events in the study region: (a) SPI and STI; (b) SPI and log(BA); (c) STI and log(BA); (d) copula-based conditional probability of log(BA) under different levels of dry and hot conditions. r is the Pearson correlation coefficient, and p denotes the significance level. Wildfires in warm (April–September) and cold (October–March) seasons are represented as red and blue dots, respectively; colored contours in (b–c) and shadings in (d) indicate the copula-based conditional probability.

(Table 1).

Figure 7 further shows the correlation between the fire intensity (FRP) and SPI and STI, and the conditional probability of wildfires with different intensities given different dry and hot conditions. Similar results are found, evidenced by the negative correlation between log(FRP) and SPI (r=–0.23, p<0.07), while a positive correlation exists between log(FRP) and STI (r=0.30, p<0.001). The wildfire intensity increased with the severity of drought and hot conditions. The conditional probability of fires with intensity like the 2025 wildfires (FRP=41 060 MW) under actual drought condition, i.e., $P[\log(FRP_{intensity})>10.6|SPI_D\leqslant-1.57]$, was 8.38%, while the conditional probability given a non-dry condition $P[\log(FRP_{intensity})>10.6|SPI_D>-0.5]$ was 5.44% (Table 1). The conditional probability under hot drought conditions, i.e., $P[\log(FRP_{intensity})>10.6|SPI_D\leqslant-1.57, STI_H>1.03]$, was 20.89%. These results indicate that the extreme drought increased the conditional probability of fires with intensity like the 2025 wildfires by 54%, and hot drought further increased the probability by 149%. Overall, relative to

Table 1. The conditional probability of wildfires with BA and FRP in 2025 under different levels of dry and hot conditions.

	Fire characteristics	Non-hot-dry conditions	Drought	Hot drought
All seasons	BA	8.06%	14.14%	43.85%
	FRP	5.44%	8.38%	20.89%
Warm seasons	BA	5.51%	7.49%	14.59%
	FRP	0.38%	1.93%	2.17%
Cold seasons	BA	3.23%	4.87%	6.32%
	FRP	7.81%	9.06%	25.39%

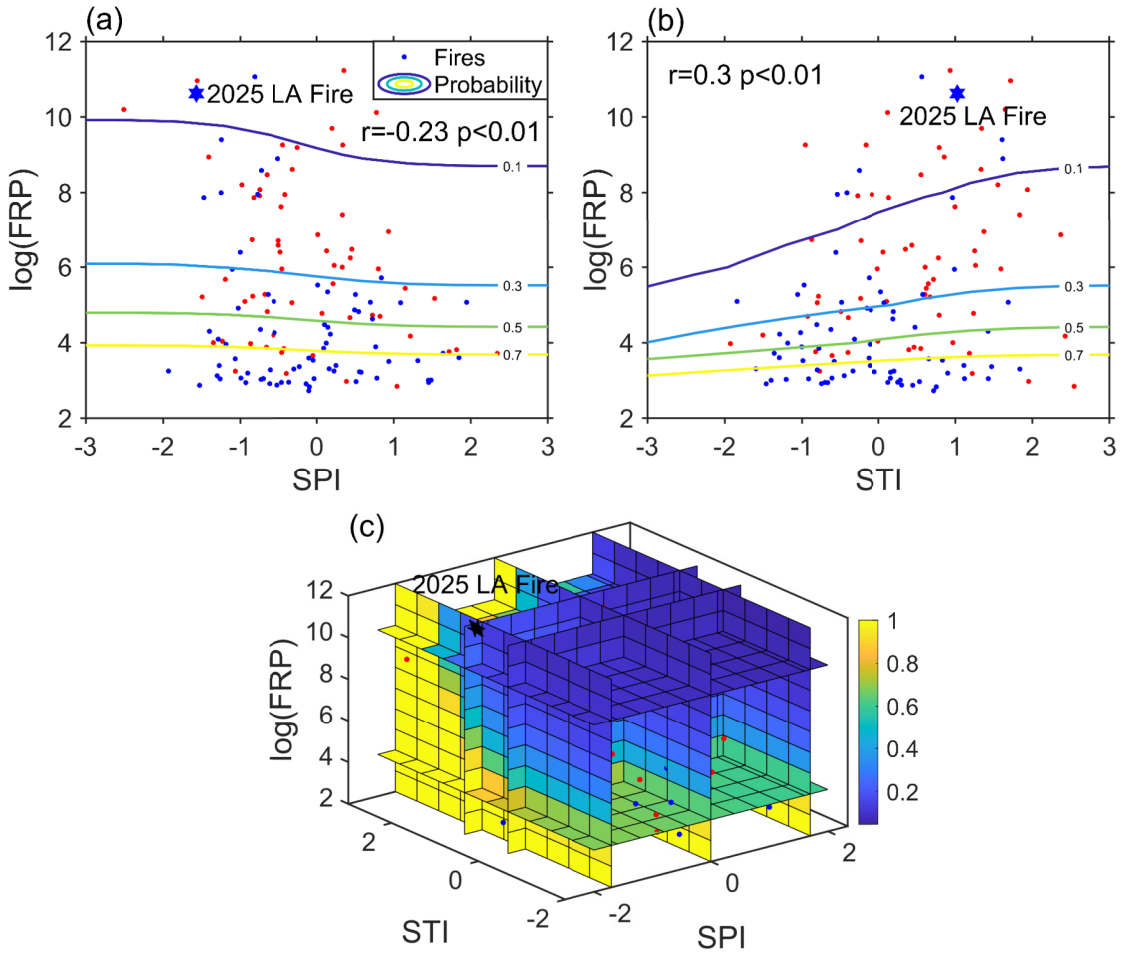

Fig. 7. Scatterplots of SPI, STI and Fire Radiative Power (FRP) for detected fire events in the study region: (a) SPI and log(FRP); (b) STI and log(FRP); (c) copula-based conditional probability of log(FRP) under different levels of dry and hot conditions. r is the Pearson correlation coefficient, and p denotes the significance level. Wildfires in warm (April–September) and cold (October–March) seasons are represented by the red and blue dots, respectively. The colored contours in (a-b) and shadings in (c) indicate the conditional probability.

a non-dry scenario, hot drought increased the likelihood of wildfires with an intensity and BA, as observed in 2025, by 2.8 and 4.4 times, respectively. The impact of hot drought conditions on fire intensity was smaller than their impact on BA.

4. Discussion

This study provides evidence that the rare 2025 LA wildfires were favored by hot drought conditions (SPI=–1.57 and STI=1.03), which dried out the vegetation, thereby providing extensive dry fuels for the wildfires. The results are consistent with previous studies that have preliminarily ascribed the 2025 wildfires to the concurrence of dry and hot conditions but did not assess their severity and impacts (Qiu et al., 2025). Here, we quantified the contribution of individual drought and hot drought to the 2025 wildfires from a probabilistic perspective. Results show that hot drought increased the conditional probability of 2025 wildfire intensity and BA by about 2.8 and 4.4 times, respectively. Despite the hot-drought amplification effect on the 2025 wildfires not being the largest historically, our analysis reveals a growing trend in its effect on BA (p<0.08) and FRP (p<0.04) (Fig. 8). This phenomenon is in agreement with previous studies that have showed an increase in the observed frequency of hot and dry extremes in California and increasing climatic potential for large wildfires (Diffenbaugh et al., 2015; Abatzoglou and Williams, 2016; Keeley and Syphard, 2021; Turco et al., 2023). Given the distinct mechanisms driving warm-season and cold-season wildfires in the western LA region, we also estimated the seasonal dependency upon the contribution of hot and drought conditions. Here, the copula relationships between wildfire characteristics and SPI and STI during the warm (April–September) and cold (October–March) seasons were fitted separately. It is found that the effects of the hot-drought conditions showed significant seasonal variations. The conditional probability of such extreme wildfires with such BA and FRP in 2025 was larger in warm and cold seasons, respectively, while the impacts of hot-drought conditions on both BA and FRP were larger in warm seasons (Table 1). This might be because more frequent hot drought conditions are conducive to fire activities

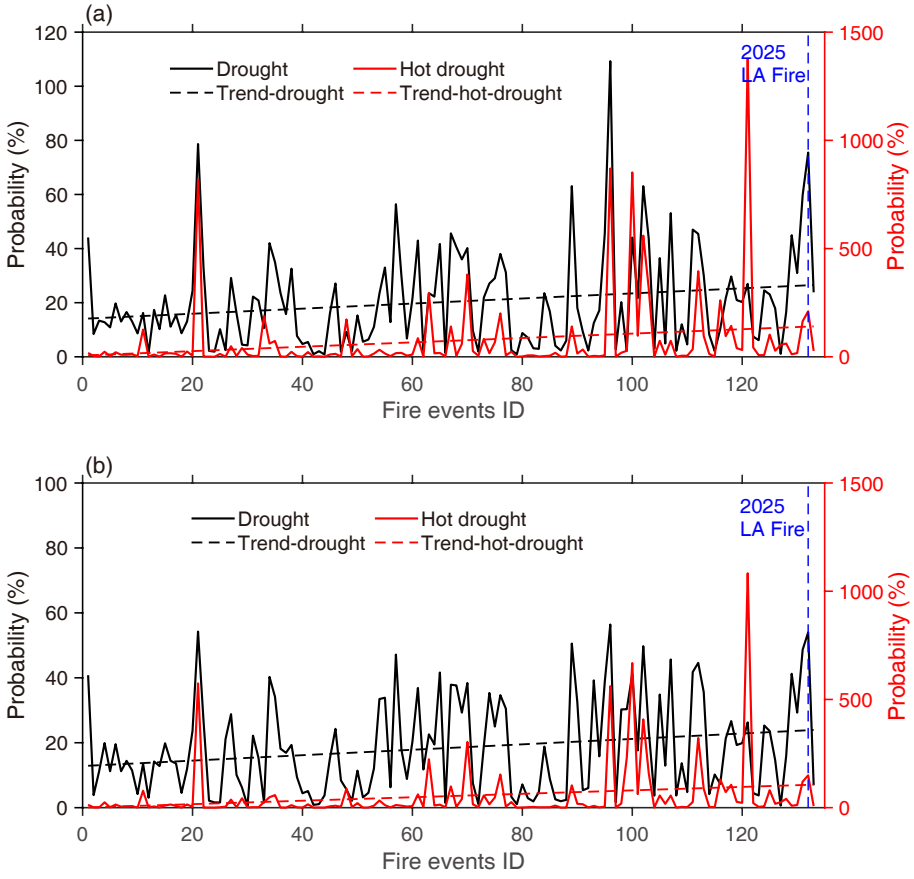

Fig. 8. The increased likelihood of the conditional probability of wildfire (a) burned area and (b) FRP given hot and dry conditions. Here, the x-axis denotes the wildfire events that occurred historically in chronological order during 2001–25. Black-solid and -dashed lines denote the increased likelihood under individual dry conditions relative to non-dry conditions and its trend, respectively. Red-solid and -dashed lines denote the increased likelihood under hot drought conditions relative to individual dry conditions and its trend, respectively. Blue-vertical lines indicate the 2025 wildfire event.

in the warm and dry seasons (Dong et al., 2022).

Although hot drought conditions have a substantial impact on fire occurrence, fuel availability plays a critical role in enhancing the fire activity (Sarris et al., 2014; Walker et al., 2020). Previous studies have shown that excessive rainfall over the previous 1–3 years has a significant impact on wildfires by promoting vegetation growth, which can provide more available fuels to burn (Pilliod et al., 2017; Li et al., 2019). Hernández Ayala et al. (2021) also suggested that more than half of the extreme wildfire seasons in California were preceded by enhanced vegetation growth due to wetter antecedent conditions. In this study, we further find that a majority of (8 of 11) extremely large wildfire cases (BA≥50 km^2), including the 2003, 2005, 2007, 2008, 2009, 2017, 2020 and 2025 wildfires, showed above average NDVI values in the peak growth season (March–May) prior to these wildfire events (Fig. 9a), indicating anomalous vegetation growth that later fueled these wildfires. Six out of the eight extreme wildfires were preceded by antecedent above-normal precipitation in the peak wet (December–February) season (Fig. 9b). The analysis for wildfires with BA>4 km^2 also reveals a significant correlation (r=0.44, p<0.01) between vegetation conditions and preceding precipitation anomalies. In this situation, the synergy between abundant fuel and local extreme weather (e.g., hot drought) may explain the very large fire spread (Pausas and Ribeiro, 2013; Gouveia et al., 2016). For the extreme wildfires without prior excessive vegetation growth (i.e., below average NDVI values), we note that the NDVI anomalies were not significant. Hot drought conditions could still drive severe burning through rapidly drying out the existing live and dead fuels (e.g., vegetation, organic soils and built structures) and reducing the ignition threshold, compounded by prolonged high vapor pressure deficit and wind-driven spread (Gouveia et al., 2016; Keeley and Syphard, 2021; Collins et al., 2022). Collins et al. (2022) have shown that very large fires usually occur in periods characterized by extreme drought and fire weather conducive to fire spread. For example, anomalous dead fuel accumulation due to prolonged drought and windblown debris fueled the 2018 megafire in California (Kang et al., 2023).

Certainly, during the extreme fire days in early January 2025, anomalous northeasterly winds with low humidity descending from elevated inland areas prevailed over the western LA region (Fig. 10a). The hourly winds exhibited a rapid strengthening at 1100 UTC (0300 PST) on 7 January, and peaked at 1900–2300 UTC (1100–1500 PST) on 7 January and 0800–1300 UTC (0000–0500 PST) on 8 January (Fig. 10b), near the time of the rapid wildfire outbreak. Under hot and dry weather conditions, the strong and dry winds usually act as a catalyst for large wildfires. For example, the anomalously dry winds can accelerate evaporation and lead to a rapid decrease in fuel moisture. Strong winds

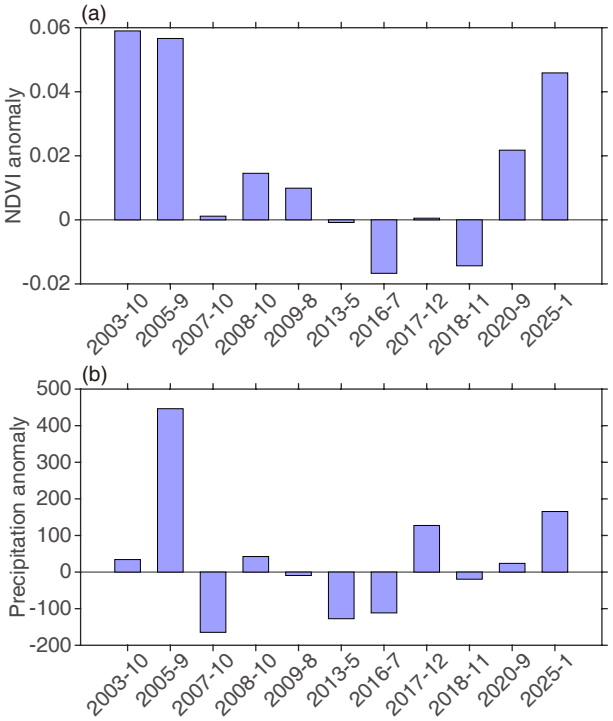

Fig. 9. Normalized Difference Vegetation Index (NDVI) and precipitation anomalies preceding the extremely large wildfire events (BA≥50 km^2): (a) Mean NDVI anomaly in the peak growth season (March–May), and (b) cumulative precipitation anomaly (mm) in the peak wet season (December–February) prior to the extreme wildfires. The x-axis represents the occurrence timeline of extremely large wildfires in the western LA region.

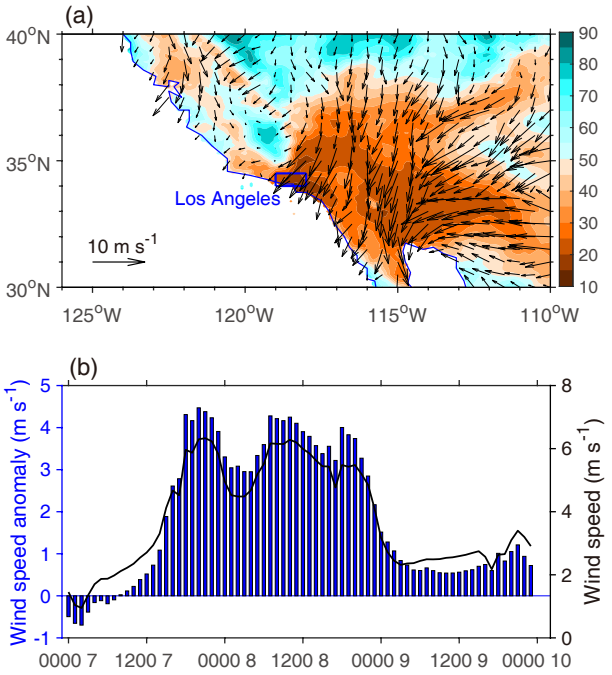

Fig. 10. (a) 10-m wind anomalies (vectors; m s^{-1}) and 2-m relative humidity (shading; %) on the peak wildfire day (i.e., 8 January 2025). Blue box denotes the western LA region. (b) Hourly (UTC) wind speed (black line; m s^{-1}) and its anomalies (blue bars; m s^{-1}) averaged over the study area during 7–9 January 2025.

can also foster the fire spread, often leading to erratic and uncontrollable fire behavior, especially during hot and dry conditions (Westerling et al., 2004; Jin et al., 2014; Qian et al., 2021). Previous studies additionally showed that hot Santa Ana winds could result in low relative humidity at the coast and preferentially favor wildfire growth (Dong et al., 2021; Gershunov et al., 2021). Therefore, the probability of such extreme wildfires might be lower in the absence of the strong and dry winds. To quantify the role of the winds in exacerbating the extreme wildfires, we partitioned wildfires into those with positive wind anomalies (W+) and those without (W-) and then evaluated the copula-based relationship between wildfires and weather conditions separately. Under hot drought conditions, the conditional probabilities of wildfires with intensity and BA in 2025 were 4.26% and 3.87% for the W- scenario, while these probabilities were 9.31% and 18.85% for W+ scenario, respectively. This indicates that concurrent windy weather had amplified the likelihood of 2025 wildfire intensity and BA by 119% and 387%, respectively.

5. Conclusions

Beginning on 7 January 2025, the western Los Angeles (LA) region experienced several large wildfires, leading to destructive social, economic, and environmental impacts. Although the burned area (~245 km^2) and intensity (FRP= 41 060 MW) were not the largest in western LA's history, the 2025 wildfires were extremely rare in terms of their extent and occurrence during the rainy (non-fire-prone) season. The wildfires ranked first in the non-traditional fire season since satellite records began in 2001, and were estimated to be at least a once-in-a-67-year event. The occurrence of the wildfires was accompanied by hot drought conditions, characterized by mean SPI and STI values of –1.57 and 1.03 during the fire period. Subsequently, we further quantified the roles of the hot drought conditions by estimating the conditional probabilities of the 2025 wildfires under non-dry, individual drought, and hot drought conditions using a copula-based Bayesian probability framework. Analysis of wildfires across all seasons shows that extreme drought during the fire period increased the probabilities of extreme wildfires with an intensity and BA in 2025 by 54% and 75% respectively. When compounded by hot drought conditions, these probabilities were further amplified by 149% for intensity and 210% for BA. The impact of hot drought was larger in warm seasons. In addition to hot drought conditions, abundant vegetation, promoted by above-average precipitation during the late winters of 2023 and 2024, and strong winds with low humidity also contributed to the extreme wildfires.

Competing interests. The authors declare that they have no competing interests.

Acknowledgements. This work was supported by the National Natural Science Foundation of China (Grant Nos. 42471034, 42330604) and the Qing Lan Project. We acknowledge the high-performance computing support from the National Key Scientific and Technological Infrastructure project "Earth System Numerical Simulation Facility" (EarthLab).

REFERENCES

Abatzoglou, J. T., and A. P. Williams, 2016: Impact of anthropogenic climate change on wildfire across western US forests. *Proceedings of the National Academy of Sciences of the United States of America*, **113**(42), 11 770–11 775, https://doi.org/10.1073/pnas.1607171113.

Abatzoglou, J. T., A. P. Williams, L. Boschetti, M. Zubkova, and C. A. Kolden, 2018: Global patterns of interannual climate–fire relationships. *Global Change Biology*, **24**, 5164–5175, https://doi.org/10.1111/gcb.14405.

Alduchov, O. A., and R. E. Eskridge, 1996: Improved Magnus form approximation of saturation vapor pressure. *Journal of Applied Meteorology and Climatology*, **35**(4), 601–609, https://doi.org/10.1175/1520-0450(1996)035<0601:IMFAOS>2.0.CO;2.

Ballarin, A. S., G. L. Barros, M. C. M. Cabrera, and E. C. Wendland, 2021: A copula-based drought assessment framework considering global simulation models. *Journal of Hydrology: Regional Studies*, **38**, 100970, https://doi.org/10.1016/j.ejrh.2021.100970.

Beck, H. E., and Coauthors, 2021: Evaluation of 18 satellite- and model-based soil moisture products using in situ measurements from 826 sensors. *Hydrology and Earth System Sciences*, **25**, 17–40, https://doi.org/10.5194/hess-25-17-2021.

Brown, P. T., H. Hanley, A. Mahesh, C. Reed, S. J. Strenfel, S. J. Davis, A. K. Kochanski, and C. B. Clements, 2023: Climate warming increases extreme daily wildfire growth risk in California. *Nature*, **621**, 760–766, https://doi.org/10.1038/s41586-023-06444-3.

Burton, C. A., S. W. Rifai, L. J. Renzullo, and A. I. J. M. Van Dijk, 2024: Enhancing long-term vegetation monitoring in Australia: A new approach for harmonising the advanced very high resolution radiometer normalised-difference vegetation index (NVDI) with MODIS NDVI. *Earth System Science Data*, **16**(10), 4389–4416, https://doi.org/10.5194/essd-16-4389-2024.

Collins, L., H. Clarke, M. F. Clarke, S. C. M. Gausden, R. H. Nolan, T. Penman, and R. Bradstock, 2022: Warmer and drier conditions have increased the potential for large and severe fire seasons across south-eastern Australia. *Global Ecology and Biogeography*, **31**, 1933–1948, https://doi.org/10.1111/geb.13514.

Diffenbaugh, N. S., D. L. Swain, and D. Touma, 2015: Anthropogenic warming has increased drought risk in California. *Proceedings of the National Academy of Sciences of the United States of America*, **112**, 3931–3936, https://doi.org/10.1073/pnas.1422385112.

Dong, C. Y., and Coauthors, 2022: The season for large fires in Southern California is projected to lengthen in a changing climate. *Communications Earth & Environment*, **3**, 22, https://doi.org/10.1038/s43247-022-00344-6.

Dong, L., L. R. Leung, Y. Qian, Y. F. Zou, F. F. Song, and X. D. Chen, 2021: Meteorological environments associated with California wildfires and their potential roles in wildfire changes during 1984–2017. *Journal of Geophysical Research: Atmospheres*, **126**, e2020JD033180, https://doi.org/10.1029/

2020JD033180.

Feng, S. F., Z. C. Hao, X. Zhang, and F. H. Hao, 2019: Probabilistic evaluation of the impact of compound dry-hot events on global maize yields. *Science of the Total Environment*, **689**, 1228–1234, https://doi.org/10.1016/j.scitotenv.2019.06.373.

Funk, C. C., and Coauthors, 2014: A quasi-global precipitation time series for drought monitoring. USGS Data Series 832, 4 pp, https://doi.org/10.3133/ds832.

Fusco, E. J., J. T. Finn, J. T. Abatzoglou, J. K. Balch, S. Dadashi, and B. A. Bradley, 2019: Detection rates and biases of fire observations from MODIS and agency reports in the conterminous United States. *Remote Sensing of Environment*, **220**, 30–40, https://doi.org/10.1016/j.rse.2018.10.028.

Gershunov, A., and Coauthors, 2021: Hot and cold flavors of southern California's Santa Ana winds: Their causes, trends, and links with wildfire. *Climate Dynamics*, **57**, 2233–2248, https://doi.org/10.1007/s00382-021-05802-z.

Giglio, L., W. Schroeder, and C. O. Justice, 2016: The collection 6 MODIS active fire detection algorithm and fire products. *Remote Sensing of Environment*, **178**, 31–41, https://doi.org/10.1016/j.rse.2016.02.054.

Giglio, L., J. Descloitres, C. O. Justice, and Y. J. Kaufman, 2003: An enhanced contextual fire detection algorithm for MODIS. *Remote Sensing of Environment*, **87**, 273–282, https://doi.org/10.1016/S0034-4257(03)00184-6.

Gouveia, C. M., I. Bistinas, M. L. R. Liberato, A. Bastos, N. Koutsias, and R. Trigo, 2016: The outstanding synergy between drought, heatwaves and fuel on the 2007 Southern Greece exceptional fire season. *Agricultural and Forest Meteorology*, **218–219**, 135–145, https://doi.org/10.1016/j.agrformet.2015.11.023.

Hao, Y., Z. C. Hao, Y. S. Fu, S. F. Feng, X. Zhang, X. Y. Wu, and F. H. Hao, 2021: Probabilistic assessments of the impacts of compound dry and hot events on global vegetation during growing seasons. *Environmental Research Letters*, **16**, 074055, https://doi.org/10.1088/1748-9326/ac1015.

Hao, Z. C., and A. AghaKouchak, 2013: Multivariate standardized drought index: A parametric multi-index model. *Advances in Water Resources*, **57**, 12–18, https://doi.org/10.1016/j.advwatres.2013.03.009.

Hawbaker, T. J., V. C. Radeloff, A. D. Syphard, Z. L. Zhu, and S. I. Stewart, 2008: Detection rates of the MODIS active fire product in the United States. *Remote Sensing of Environment*, **112**(5), 2656–2664, https://doi.org/10.1016/j.rse.2007.12.008.

Hernández Ayala, J. J., J. Mann, and E. Grosvenor, 2021: Antecedent rainfall, excessive vegetation growth and its relation to wildfire burned areas in California. *Earth and Space Science*, **8**(9), e2020EA001624, https://doi.org/10.1029/2020EA001624.

Jiang, T. L., X. L. Su, G. X. Zhang, T. Zhang, and H. J. Wu, 2023: Estimating propagation probability from meteorological to ecological droughts using a hybrid machine learning copula method. *Hydrology and Earth System Sciences*, **27**, 559–576, https://doi.org/10.5194/hess-27-559-2023.

Jin, Y. F., J. T. Randerson, N. Faivre, S. Capps, A. Hall, and M. L. Goulden, 2014: Contrasting controls on wildland fires in Southern California during periods with and without Santa Ana winds. *Journal of Geophysical Research: Biogeosciences*, **119**, 432–450, https://doi.org/10.1002/2013JG002541.

Kang, Z. Y., X. W. Quan, and G. K. Lai, 2023: Assessing the effects of fuel moisture content on the 2018 Megafires in California. *IEEE Journal of Selected Topics in Applied Earth Observations and Remote Sensing*, **16**, 868–877, https://doi.org/10.1109/JSTARS.2022.3232665.

Keeley, J. E., and A. D. Syphard, 2021: Large California wildfires: 2020 fires in historical context. *Fire Ecology*, **17**, 22, https://doi.org/10.1186/s42408-021-00110-7.

Khorshidi, M. S., P. E. Dennison, M. R. Nikoo, A. AghaKouchak, C. H. Luce, and M. Sadegh, 2020: Increasing concurrence of wildfire drivers tripled megafire critical danger days in Southern California between1982 and 2018. *Environmental Research Letters*, **15**, 104002, https://doi.org/10.1088/1748-9326/ABAE9E.

Li, A. X., Y. Wang, and Y. L. Yung, 2019: Inducing factors and impacts of the October 2017 California wildfires. *Earth and Space Science*, **6**(8), 1480–1488, https://doi.org/10.1029/2019EA000661.

Li, Y. F., and Coauthors, 2023: Warming and greening exacerbate the propagation risk from meteorological to soil moisture drought. *Journal of Hydrology*, **622**, 129716, https://doi.org/10.1016/j.jhydrol.2023.129716.

Libonati, R., and Coauthors, 2022: Assessing the role of compound drought and heatwave events on unprecedented 2020 wildfires in the Pantanal. *Environmental Research Letters*, **17**, 015005, https://doi.org/10.1088/1748-9326/ac462e.

Littell, J. S., 2018: Drought and fire in the Western USA: Is climate attribution enough?. *Current Climate Change Reports*, **4**, 396–406, https://doi.org/10.1007/s40641-018-0109-y.

Liu, Y. C., Z. Li, Y. N. Chen, Y. P. Li, H. W. Li, Q. Q. Xia, and P. M. Kayumba, 2022: Evaluation of consistency among three NDVI products applied to High Mountain Asia in 2000–2015. *Remote Sensing of Environment*, **269**, 112821, https://doi.org/10.1016/j.rse.2021.112821.

Ma, B., X. P. Liu, Z. J. Tong, J. Q. Zhang, and X. Wang, 2024: Coupled effects of high temperatures and droughts on forest fires in Northeast China. *Remote Sensing*, **16**, 3784, https://doi.org/10.3390/rs16203784.

Ma, F., and X. Yuan, 2024: Vegetation greening and climate warming increased the propagation risk from meteorological drought to soil drought at subseasonal timescales. *Geophysical Research Letters*, **51**, e2023GL107937, https://doi.org/10.1029/2023GL107937.

Ma, F., L. F. Luo, A. Z. Ye, and Q. Y. Duan, 2019: Drought characteristics and propagation in the semiarid Heihe River basin in Northwestern China. *Journal of Hydrometeorology*, **20**, 59–77, https://doi.org/10.1175/JHM-D-18-0129.1.

McKee, T. B., N. J. Doesken, and J. Kleist, 1993: The relationship of drought frequency and duration to time scales. *Eighth Conference on Applied Climatology*, Anaheim, California, American Meteorological Society, 179–184.

Muñoz-Sabater, J., and Coauthors, 2021: ERA5-Land: A state-of-the-art global reanalysis dataset for land applications. *Earth System Science Data*, **13**, 4349–4383, https://doi.org/10.5194/essd-13-4349-2021.

Pausas, J. G., and E. Ribeiro, 2013: The global fire–productivity relationship. *Global Ecology and Biogeography*, **22**, 728–736, https://doi.org/10.1111/geb.12043.

Pilliod, D. S., J. L. Welty, and R. S. Arkle, 2017: Refining the cheatgrass-fire cycle in the Great Basin: Precipitation timing and fine fuel composition predict wildfire trends. *Ecology and Evolution*, **7**(19), 8126–8151, https://doi.org/10.1002/ece3.3414.

Qian, W. H., Y. Ai, J. Y. Yu, and J. Du, 2021: Opposite anomalous synoptic patterns for potential California large wildfire spread and extinguishing in 2018 cases. *Atmospheric Research*, **262**, 105804, https://doi.org/10.1016/j.atmosres.2021.105804.

Qiu, M. H., D. Y. Chen, M. Kelp, J. Li, G. Y. Huang, and M. D. Yazdi, 2025: The rising threats of wildland-urban interface fires in the era of climate change: The Los Angeles 2025 fires. *The Innovation*, **6**(5), 100835, https://doi.org/10.1016/j.xinn.2025.100835.

Ribeiro, A. F. S., A. Russo, C. M. Gouveia, P. Páscoa, and J. Zscheischler, 2020: Risk of crop failure due to compound dry and hot extremes estimated with nested copulas. *Biogeosciences*, **17**, 4815–4830, https://doi.org/10.5194/bg-17-4815-2020.

Sadegh, M., E. Ragno, and A. AghaKouchak, 2017: Multivariate Copula Analysis Toolbox (MvCAT): Describing dependence and underlying uncertainty using a Bayesian framework. *Water Resources Research*, **53**, 5166–5183, https://doi.org/10.1002/2016WR020242.

Sarris, D., A. Christopoulou, E. Angelonidi, N. Koutsias, P. Z. Fulé, and M. Arianoutsou, 2014: Increasing extremes of heat and drought associated with recent severe wildfires in southern Greece. *Regional Environmental Change*, **14**, 1257–1268, https://doi.org/10.1007/s10113-013-0568-6.

Seager, R., A. Hooks, A. P. Williams, B. Cook, J. Nakamura, and N. Henderson, 2015: Climatology, variability, and trends in the U.S. vapor pressure deficit, an important fire-related meteorological quantity. *Journal of Applied Meteorology and Climatology*, **54**, 1121–1141, https://doi.org/10.1175/JAMC-D-14-0321.1.

Sheridan, S. C., C. C. Lee, and E. T. Smith, 2020: A comparison between station observations and reanalysis data in the identification of extreme temperature events. *Geophysical Research Letters*, **47**, e2020GL088120, https://doi.org/10.1029/2020GL088120.

Shi, Z. T., D. B. Jiang, and Y. L. Wang, 2024: Spatiotemporal dependence of compound drought–heatwave and fire activity in China. *Weather and Climate Extremes*, **45**, 100695, https://doi.org/10.1016/j.wace.2024.100695.

Svoboda, M., and Coauthors, 2002: The drought monitor. *Bulletin of the American Meteorological Society*, **83**(8), 1181–1192, https://doi.org/10.1175/1520-0477-83.8.1181.

Swain, D. L., 2021: A shorter, sharper rainy season amplifies California wildfire risk. *Geophysical Research Letters*, **48**, e2021GL092843, https://doi.org/10.1029/2021GL092843.

Turco, M., J. T. Abatzoglou, S. Herrera, Y. Z. Zhuang, S. Jerez, D. D. Lucas, A. AghaKouchak, and I. Cvijanovic, 2023: Anthropogenic climate change impacts exacerbate summer forest fires in California. *Proceedings of the National Academy of Sciences of the United States of America*, **120**(25), e2213815120, https://doi.org/10.1073/PNAS.2213815120.

Walker, X. J., and Coauthors, 2020: Fuel availability not fire weather controls boreal wildfire severity and carbon emissions. *Nature Climate Change*, **10**, 1130–1136, https://doi.org/10.1038/s41558-020-00920-8.

Wang, Z. X., L. H. Ke, and F. P. Deng, 2011: Doubling MODIS-NDVI temporal resolution: From 16-Day to 8-Day. *Remote Sensing Technology and Application*, **26**(4), 437–443. (in Chinese with English abstract)

Westerling, A. L., H. G. Hidalgo, D. R. Cayan, and T. W. Swetnam, 2006: Warming and earlier spring increase western U.S. forest wildfire activity. *Science*, **313**, 940–943, https://doi.org/10.1126/science.1128834.

Westerling, A. L., D. R. Cayan, T. J. Brown, B. L. Hall, and L. G. Riddle, 2004: Climate, Santa Ana winds and autumn wildfires in southern California. *Eos, Transactions American Geophysical Union*, **85**, 289–296, https://doi.org/10.1029/2004EO310001.

Wu, H. J., X. L. Su, V. P. Singh, K. Feng, and J. P. Niu, 2021: Agricultural drought prediction based on conditional distributions of Vine Copulas. *Water Resources Research*, **57**, e2021WR029562, https://doi.org/10.1029/2021WR029562.

Yang, H. Y., F. Ma, X. Yuan, P. Ji, and C. Y. Li, 2025: Vegetation greening accelerated the propagation from meteorological to soil droughts in the Loess Plateau from a three-dimensional perspective. *Journal of Hydrology*, **650**, 132522, https://doi.org/10.1016/j.jhydrol.2024.132522.